**RESEARCH ARTICLE**

Elemental Bioimaging by Means of Fast Scanning Laser Ablation-Inductively Coupled Plasma-Mass Spectrometry

Christoph A. Wehe,[1] Georgina M. Thyssen,[1] Christina Herdering,[1] Indra Raj,[2]
Giuliano Ciarimboli,[2] Michael Sperling,[1,3] Uwe Karst[1]

[1]Institute of Inorganic and Analytical Chemistry, University of Münster, Corrensstr. 28/30, 48149, Münster, Germany
[2]University of Münster, University Hospital, Medical Clinic D, Experimental Nephrology and Interdisciplinary Center for Clinical Research (IZKF), Albert-Schweitzer-Campus 1 – A14, 48149, Münster, Germany
[3]European Virtual Institute for Speciation Analysis (EVISA), Mendelstr. 11, 48149, Münster, Germany
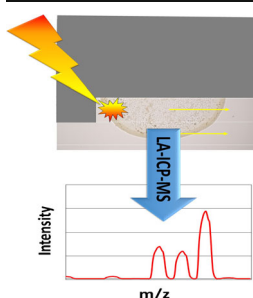
Abstract. One of the most common setups for elemental bioimaging, the hyphenation of a laser ablation (LA) system and an inductively coupled plasma mass spectrometer (ICP-MS), was expanded by adding full scan mass spectrometric information as another dimension of information. While most studies deal with the analysis of typically not more than up to 10 isotopes per scan cycle, a fast scanning quadrupole mass analyzer was utilized to record the full mass spectrum of interest in this work. Mass-to-charge ratios from 6 to 250 were observed within one cycle. Besides the x- and y-position on the ablated sample and the intensity, the *m/z*-ratio served as fourth variable for each pixel of the obtained data, closing thereby the gap between "inorganic" and "organic" mass spectrometric imaging techniques. The benefits of this approach include an improved control of interferences, the discovery of unexpected elemental distributions, the possibility to plot isotopic ratios, and to integrate the intensities of a certain number of mass channels recorded for each isotope, thus virtually increasing sensitivity. The respective data are presented for dried droplets as well as embedded animal and human tissue slices. Limits of detection were calculated and found to be in accordance with counting statistics. A dedicated software macro was developed for data manipulation prior to common evaluation and image creation.

Keywords: Elemental bioimaging, Laser ablation, Inductively coupled plasma-mass spectrometry (ICP-MS), Rapid scanning

Introduction

In recent years, elemental bioimaging has gained more and more importance owing to the increasing importance of life sciences and to instrumental improvements [1–3]. One of the most important techniques for this purpose is the combination of laser ablation (LA) and inductively coupled plasma mass spectrometer (ICP-MS), either equipped with a quadrupole (QP) or with a sector field (SF) mass analyzer [4, 5]. A spatial resolution down to 2–4μm for commercially available instruments and limits of detection in the low ng/g range may be achieved owing to the high sensitivity and low background noise for detecting most elements of the periodic table. LA-ICP-MS has therefore become a versatile tool for the life sciences [6–8].

However, there are still major challenges remaining for this technology: spatial resolution still needs to be improved, and increased sensitivity is required to sustain low limits of detection for decreasing amounts of sample. Once the sample is ablated and subsequently transported by a carrier gas (He and Ar) to the ICP-MS for vaporization, atomization, and ionization, it cannot be analyzed a second time. This is particularly problematic if the investigated analyte is not free from spectral polyatomic interferences deriving from the plasma gas or when drift effects occurred during analysis, although interferents may be utilized as internal standards in order to overcome drift effects [9, 10].

Correspondence to: Uwe Karst; *e-mail:* uk@uni-muenster.de

Thus, it would be superior to acquire signals of all elements, or at least all elements that could be of further interest, in one single run and to have a full mass spectrum available for each acquired pixel [11]. In the field of "organic" mass spectrometric imaging, with matrix assisted laser desorption ionization (MALDI) as its common ionization technique, this is achieved for example by utilization of Orbitrap [12] or time of flight (ToF) [13] mass analyzers. However, these techniques suffer from a lack of simple quantitation capabilities compared with ICP-based approaches. Nevertheless, "inorganic" mass spectrometry struggles to cope with short transient signals, and different dedicated approaches have been proposed to overcome this issue in LA-ICP-MS [11, 14–16].

Single-collector sector field instruments in the straight or reversed Nier-Johnson geometry are limited in their scan speed across the entire mass region of interest owing to the settling time of the utilized electromagnet and the field regulator. A fast scan of the electrostatic analyzer (ESA) in conjunction with changes in the acceleration voltage is only possible in a mass range of about +30% from the adjusted m/z of the magnet. This combination does not show better sensitivity compared with modern quadrupole instruments. Instruments using a line of direct-charge-detectors (DCD) or Faraday-strip array detectors in the Mattauch-Herzog geometry are, in theory, capable of recording the complete "inorganic" m/z range simultaneously [6, 17]. However, these techniques suffer from comparably poor limits of detection (LOD) and a lack of robustness. Therefore, multi-collector instruments remain the gold standard for high-precision isotopic ratio determinations [18–21].

For this reason, another fast scanning technique, widely applied in "organic" mass spectrometry, was evaluated as a detection system for LA-ICP-MS in 1996 [22]; early commercial systems could not compete with quadrupole systems with respect to detection power and duty cycle. Günther et al. [23] recently published several articles about the construction and application of an ICP-TOF-MS instrument. It is mainly used for the analysis of nanoparticles and overcomes the typical issues of former instrument generations, including the inferior time resolution, which is due to the necessity to sum hundreds of spectra to improve the signal to noise ratio (S/N). Bandura et al. described the development and application of a recently commercialized ICP-ToF-MS for the analysis of single cells tagged with rare earth elemental labels (CyTOF). The instrument is able to acquire a mass spectrum from m/z 125 to 215 in 13μs, resulting in a scan speed of 76.8MHz [24].

For the analysis of nanoparticles in the "single particle mode," the sample is highly diluted, and individual particles are recorded as spikes. The number of spikes is proportional to the concentration of particles, and the intensity of each spike corresponds to the particle size. For this work, short dwell times in the range of a few milliseconds are required, whereas the visualization of the generated ion cloud calls for dwell times of 100μs or less [25, 26]. Even if this is possible with some commercially available instruments, the delay between consecutive scan cycles prevents its application. Therefore, oscilloscopes have been used to read out the signals of the secondary electron multiplier detectors [27]. The same considerations are valid for single-shot LA experiments [28]. For the hyphenation of gas chromatography (GC) and MS, the use of the second stability region of the Mathieu diagram has been discussed, allowing scan speeds of up to 1000Hz for an m/z region of 80, but this suffers from poor sensitivity compared with region one and mass aliasing [29]. Hence, short transient signals remain a challenge for elemental mass spectrometry [30–32].

In this work, a new approach is presented to close the gap between detection schemes used for "inorganic" and "organic" mass spectrometry: data acquisition by continuous sweeping or fast jumping over the complete m/z range of interest. This technique is widely applied in quadrupole-based ICP-MS instead of the conventional peak-hopping mode with the goal to reveal spectral interferences and unexpected matrix components as well as for semiquantitative data evaluation. Here, the sensitivities for all analytes present in the external calibration are plotted against the corresponding m/z value after correction for isotopic abundances. This fast scan provides several other unique benefits, especially for transient signals generated by hyphenated techniques, including LA-ICP-MS, considering that the settle time of the quadrupole depends on the width of the mass jump over the mass region of interest. Further advantages are the enhancement of sensitivity by summation of mass channels as well as the possibility of generating mass ratio and interferences plots. These will be discussed and utilized for different applications, including the analysis of dried droplets and thin tissue slices of animal or human origin. Additionally, a simple Visual Basic for Applications (VBA) macro is presented for data handling.

Experimental

Instrumentation

An inductively coupled plasma mass spectrometer of the most recent generation (iCAP Qc; Thermo Fisher Scientific, Bremen, Germany), equipped with a quadrupole mass analyzer and a flatapole-based collision/reaction cell (QCell) was used throughout all studies. Owing to the possible formation of unwanted polyatomic spectral interferences, the high sensitivity kinetic energy discrimination mode (KEDS) of the ICP-MS system was utilized with an energy barrier of 3V between the cell and the quadrupole mass analyzer. The instrument was operated at a power of 1550W (free-running generator), a cool gas flow of 14L/min, and an auxiliary gas flow of 0.5–0.8L/min. The sampling depth was set to 5–7mm. Helium (99.999% purity) served as collision gas for all studies involving dried coffee and whole blood samples, and a mixture of 6% (v/v) H_2 in He (99.999% purity) was used for all other experiments. The cell gas flow and the lenses in front and behind the collision/reaction cell were adjusted on a daily basis using a Co standard solution with a concentration of 1μg/L in 2% (w/w) HNO_3 and 0.5% (w/w) HCl. The cell gas flow was set to give a $^{59}Co/^{35}Cl^{16}O$ ratio >25. This resulted in flow values of 4.2mL/min for pure He and 5.9mL/min for the gas mixture.

The utilized laser ablation system (LSX-213; Teledyne CETAC Technologies Inc., Omaha, NE, USA) was based on a frequency-quintupled, Q-switched Nd:YAG laser and coupled to the ICP-MS by means of a PTFE-coated Tygon tube.

Critical laser parameters, including laser energy and shot repetition rate, were adjusted according to the utilized scan rate in order to ablate the investigated material quantitatively in a multiline scan with no gap between the lines. Detailed parameters are given in the corresponding sections. The scan speed of the ablation stage was set to produce one pixel per second in the final image to simplify image processing and to improve comparability between different studies. Only for the coffee droplet studies, the scan speed was adjusted based on the set dwell time to show the influence of the quadrupole settling. Special attention was paid to the formation of debris, as a re-ablation would distort the obtained elemental images. A cylindrical ablation chamber with sample insert was used to reduce the inner volume of the cell to approximately $25cm^3$, resulting in combined washout and transport times in the range of 1.8–2.2s, whereas the washout time of the cell itself was in the range of 0.9s. To achieve these values, a He flow of 0.7L/min was used to flush the generated aerosol from the ablation cell to the ICP-MS. Coupling of the instruments was performed using a home-built dual sample inlet in which the aerosol from the laser ablation is mixed with the tertiary aerosol, generated by a µFlow-PFA nebulizer (Elemental Scientific Inc., Omaha, NE, USA). The cyclonic quartz glass spray chamber was cooled to 2.7°C. This dual mode approach has two major advantages. First, it facilitates the tuning procedure: the x- and y-position of the torch, the nebulizer gas flow, the potential of the second extraction lens, and the lens in front of the QCell were tuned on a daily basis by introducing a multi-element standard with a sensitivity for 1µg/L of at least 350,000 cps, an oxide ratio of <0.01 (measured as ^{140}Ce oxide), and a doubly charged ratio of <0.03 (measured on ^{137}Ba), with all other gas flows set as described. Typical nebulizer flow values were in the range of 0.7L/min for a 3.5mm injector pipe. In each case, Ni sampler and skimmer cones were used, the latter equipped with an insert length of 2.8mm. Second, the dual mode approach allows for a constant monitoring of the instrument's sensitivity. For all studies, the relative standard deviations (RSDs) were well below 5% for the complete runs.

Macroinstruction files were written using Microsoft (Redmond, WA, USA) Excel 2013 VBA and Microsoft Visual Studio Professional 2013 in order to handle the raw data. The ICP-MS was controlled using the Qtegra ISDS 1.7 software (Thermo Fisher Scientific, Bremen, Germany). The exported CSV files were transformed into images using ImageJ 1.46r (Wayne Rasband, http://imagej.nih.geov/ij). Histograms were plotted using Origin Pro 8 SR2 (OriginLab, Northampton, MA, USA).

Materials

Elemental standards (1000mg/L) were ordered from VHG Labs (Manchester, NH, USA). Nitric acid (suprapure, 65%) was purchased from Merck (Darmstadt, Germany). Paraplast X-TRA (melting point 52°C) and Surgipath Paraplast (melting point 56°C) were purchased from Leica Biosystems (Wetzlar, Germany). Roti-Histofix (4% formaldehyde in phosphate buffer) was obtained from Carl Roth (Karlsruhe, Germany). Superfrost Plus adhesive microscope slides were purchased from Thermo Fisher Scientific (Waltham, MA, USA). Isobutanol was obtained from Amresco (Solon, OH, USA) and ethanol from AppliChem (Darmstadt, Germany). For lymph node tissue section preparation, formaldehyde was purchased from H. Möller (Steinfurt, Germany), ethanol and xylene from Kassner and Sasse (Dortmund, Germany), Certistain eosin Y C.I. from Merck. Water was freshly purified through an Aquatron Water Stills purification system model A4000D (Barloworld Scientific, Nemours Cedex, France). All chemicals were used in the highest purity available.

FVB/N HanHsd mice (Harlan Laboratories, Horst, The Netherlands) were grown in the animal facilities of the University Hospital of Münster. Cisplatin [cis-diamminedichloridoplatinum(II), CDDP] treatment was carried out with a 8×4mg/kg delivery over 8 wk. The animals were sacrificed 7 wk later. Experiments were approved by a governmental committee on animal welfare (LaNUV, permission number A 140.2011) and performed in accordance with national animal protection guidelines. Perfusion, fixation, staining, and embedding of the tissue sample before sectioning to 3µm was done as described recently [33]. Lymph node samples were obtained from anonymized human patients as a waste product after surgeries and prepared to 8-µm-thick sections as described elsewhere [33]. Human whole blood was taken from a healthy volunteer.

Results and Discussion

General Considerations

The spatial resolution of an image is adjustable for the y-direction via the laser spot diameter focused onto the sample. However, the maximum feed rate of the laser beam in the x-direction in a line-by-line scan is typically limited by the washout time of the ablation cell and the scan speed of the quadrupole mass analyzer. Currently, the maximum number of pixels that can be recorded per second seems to be in the region of 4Hz [34]. This also means that if one is interested in only one analyte, the dwell time of the quadrupole is adjusted in this case to f=0.25s, whereas the settle times of the quadrupole are not taken into account. Thus, the dwell time is set to 1/f. The electronics of commercially available quadrupole systems are able to scan the mass analyzer much faster than this and, hence, not only one but a variety of analytes of interest are typically selected for elemental bioimaging studies. Thus, the equation can be adapted to 1/(j*c*f), where j is the number of analytes and c is the number of channels for one mass peak. Typically, not more than 10 analytes are selected, even if more analytes would be favorable owing to the destructive nature of the LA technique. This results in a dwell time of 25ms in the example
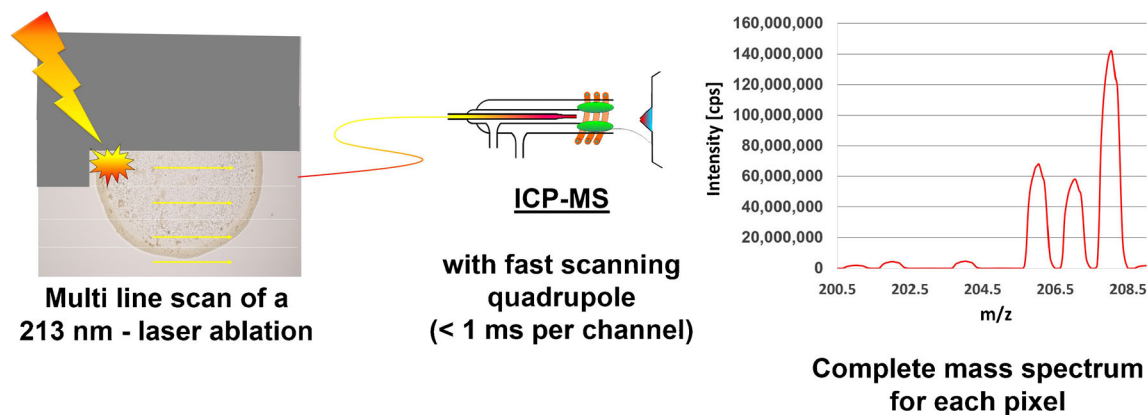
Figure 1. Schematic depiction of the fast survey scan acquisition approach: the sample is ablated in a line-by-line scan, whereas the produced dry aerosol is subsequently transported to the ICP-MS system equipped with a quadrupole mass analyzer. Owing to a fast survey scan acquisition, a complete mass spectrum for each pixel is obtained

mentioned above. However, with an increasing number of analytes, the duty cycle of the quadrupole is increasingly important. As the settle time, which is necessary for stable operation, depends on the width of the mass jump, the total scan time for, e.g., 100 channels, is not always the same, but rather depends on the selected mass region. Thus, the optimum duty cycle for a given number of mass channels is achieved if the mass window is comparably narrow. Typical values are in the range of not more than 0.2–0.5 u distance between consecutive mass channels, depending on the instrument. If one would select all isotopes that could be of particular importance for an elemental bioimaging study, most of the analysis time would be wasted to adjust the correct *m/z* value. This lowers the effective time for ion collection and, accordingly, the LODs because of poor counting statistics. Moreover, the possibility of false positive results increases because of spikes of different origin. The reason for this is that the displayed unit of the intensities is counts per second (cps), and the raw intensity within one dwell time is multiplied by the reciprocal of the dwell time. Additionally, unidentified spectral interferences may occur. Hence, a fast survey scan acquisition of the complete *m/z* region with fast jumping between the mass channels could circumvent these issues. The principle of this approach, which can be used on nearly every commercially available quadrupole ICP-MS instrument, is shown in Figure 1. It virtually adds another dimension to elemental bioimaging: the *m/z* ratio in addition to x- and y-position and the intensity of the signal. By plotting the complete *m/z* region of interest, one has a powerful tool to reveal spectral interferences and a proof for the identity of the analyte by its isotopic abundances.

Data Processing and Sensitivity Improvement

To prove if the fast scanning approach is able to provide accurate results without image distortion, a coffee droplet was spotted on a microscopic slide. After drying, the droplet was ablated in 59 line scans with a gap between the lines of 0μm, a spot size of 25μm, a laser scan rate of 50μm/s, and a laser energy of 2.9mJ/shot using a repetition rate of 20Hz. The transient survey scan covered a mass range from 22.1 to 240 u with a distance between consecutive mass channels of 0.2 u. Each channel was scanned with a dwell time of 500μs. Thus, a number of 1089 channels should be scanned within 544.5ms. However, owing to the settling time of the quadrupole, the duty cycle needed to be taken into account, which equaled 37.8% in this experiment (calculated by the exact start and stop times of each line scan) and, hence, 1.44s were needed for one scan. Figure 2 shows an example of a mass spectrum as the sum of intensities of one single line, whereas Figure 3 shows a summary of the obtained data for potassium. As can be readily seen, the image of the droplet is stretched in the x-direction because of the prolonged acquisition time, whereas in the y-direction, an accurate distance was obtained (Figure 3a). Nevertheless, refitting the size of the pixels by a factor of 0.378 in the x-direction gave a correct representation. This shows that the settling time of the quadrupole is the only effect, which needs to be taken into account for the conversion of the time scale to
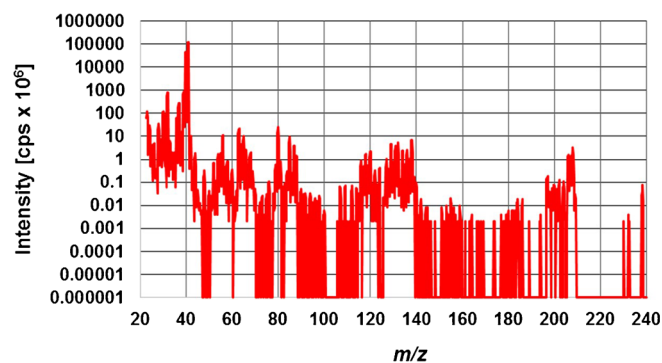
Figure 2. Mass spectrum as the sum of intensities obtained after the ablation of one single line of a dried coffee droplet. As the complete mass range of interest was recorded, the identity of the analytes can be proven by their isotopic pattern
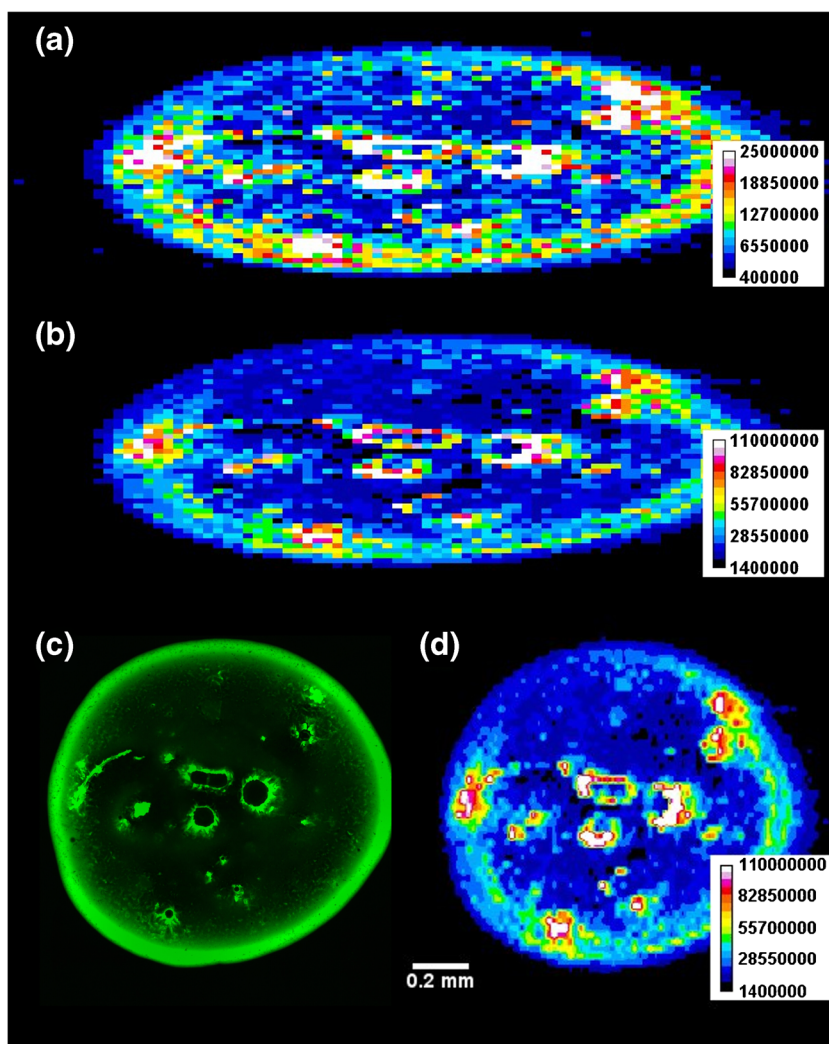
Figure 3. ^{39}K trace of a coffee droplet: image of central mass channel **(a)** and summation over 5 mass channels **(b)**, both without correction for distortion, which has its origin in the prolonged scan time of the quadrupole compared with the adjusted value. Fluorescence image of the coffee droplet **(c)**, which is in excellent agreement with the duty cycle corrected ion image **(d)**. Distortion of the obtained images was overcome by calculation of the corresponding duty cycle, whereas sensitivity was improved by summation of all mass channels for one isotope. In **(d)**, a bilinear interpolation, in which pixels with the mean value of the adjacent ones are added for both directions, was additionally used during distortion correction

the distance scale (Figure 3d). This statement was proven by comparison to a fluorescence image of the same droplet (Figure 3c) showing the same width and height as well as the same structural details completely as the potassium ion image.

The obtained sensitivity is directly proportional to the contrast of the ion images. The novel imaging technique allows adding up the different mass channels for one mass peak, e.g., five channels in this example. The approach is commonly performed on SF-instruments, thereby virtually increasing their sensitivity for every E-scan. As can be seen in Figure 3, the same effect is observed for this approach. After summation of all mass channels in the range of 38.5–39.5 u and considering that in normal resolution mode the peak width at 10% peak height (R=300) was adjusted to be<0.7 u, the sensitivity is significantly increased (Figure 3a→Figure 3b). This provides

an enhanced contrast of the final image and removes false pixel colors originating from spikes in the raw data.

Another critical aspect in recording transient signals by sequential scans is the spectral skew: when a low mass analyte like lithium is only present in the last part of an ablated voxel, which is the volume equivalent of a pixel, or a high mass analyte like uranium is only present in the first part, they may not be detected, as each voxel is scanned beginning at the lower mass side [14]. This is also valid for imaging experiments involving more than one analyte, but becomes more significant when the number of monitored analytes increases. It is therefore of particular importance to set the laser beam diameter to a sufficiently small size to represent the structure of the investigated sample. For a spiked droplet shown in Figure 3, this was already achieved using a spot size of 25μm. Adjacent pixels show only slight variations in terms of intensity. Hence, there is

no evidence that spectral skew obstructs the correct representation of elemental distributions inside a sample.

## Limits of Detection, Accuracy, and Precision in Isotopic Ratio Analyses

To investigate the effect of shortened dwell times and mass channel summation in detail, different scan parameters were tested during the ablation of NIST SRM 612–trace elements in glass. Titanium (scanned at m/z 49) was chosen as a model analyte with low isotopic abundance and high blank values, whereas thorium served as high mass analyte with superior LOD.

Owing to calculation of the intensity as counts per second, the gas blank values as well as the obtained intensities for the ablation of the standard do not vary significantly from each other for the different investigated scan settings. This is demonstrated in Table 1. The relative standard deviation (RSD) is proportional to the number of runs, when calculated for a fixed scan duration of 60s. Summation of three mass channels (spacing=0.1 u) does not influence the limits of detection, which were calculated according to the 3σ-criterion. This is because independent of the number of mass channels, the number of recorded data points and, in good approximation, the ion current hitting the secondary electron multiplier, stays the same. Hence, the results are in accordance to Poisson (counting) statistics, which can be seen by the constancy in the calculated statistical factor, which is the square root of the raw intensities times the number of scans divided by the calculated LOD. In general, imaging based on fast survey scan acquisition degrades the obtainable LODs by approximately one order of magnitude in a worst case scenario. However, this does not limit the applicability significantly when taking the current instrumental capabilities into account. Nevertheless, the results provide further evidence for the validity of mass trace summation, as sensitivity and, hence, image contrast is improved. For thorium, LODs could not be calculated, as the gas blank values for the different scan settings always equaled zero. The standard deviations for the ablation of the glass SRM were always in the same range (approximately 30%) and, hence, the fast scanning imaging approach over a wide mass range here delivered the same results compared with conventional imaging experiments monitoring only one isotope. However, the wider mass window enabled the time-resolved monitoring of oxide formation (about 5%) and thus further experiments were conducted to show the ability to obtain accurate and precise results.

Figure 4 shows an overview of the data, which were obtained by ablation of a dried human whole blood droplet, spiked with 10mg/L lead. Here, the laser parameters were set to a spot size of 25μm, a shot repetition rate of 20Hz, a scan speed of 25μm/s, and a laser energy of 1.95mJ/shot. Again, the "coffee ring" structure can be seen, e.g. for m/z 206 in (Figure 4a). However, as the mass range from 200.1 to 210.0 u was scanned with a spacing of 0.05 u between the mass channels and a dwell time of 0.005s, a region comprising all Pb isotopes could be

Table 1. Experimental limits of detection using different scan settings for ^{49}Ti in NIST SRM 612 – Trace elements in glass (reference value=50.1±0.8 mg/kg). The observed RSDs increase with the number of runs conducted within a defined time interval. The number of scanned channels per mass, here with a spacing of 0.1 u, virtually increases the sensitivity, but not the precision. Hence, the achievable LODs are in the same range for experiments involving 1 or 3 channels. The presented findings are in good agreement to Poisson statistics. [35] A calculated statistical factor (square root of the raw intensities times the number of scans divided by the calculated LOD) is almost constant for all settings

Dwell time [s]	Number of channels [-]	Number of runs [-]	Time / run [s]	I (Blank) [cps]	RSD (Blank)	I (Standard) [cps]	LOD [mg/kg]	Statistical factor
5.00000	1	12	5	125	3.3%	688	1.1	273
1.00000	1	60	1	135	6.8%	633	2.8	251
0.33333	3	60	0.999	342	9.0%	2026	2.7	233
0.05000	1	1200	0.05	121	44.0%	699	13.9	212
0.01666	3	1200	0.04998	351	43.2%	2024	13.6	213
0.00500	1	12000	0.005	120	133.6%	709	41.0	227
0.00166	3	12000	0.00498	364	137.3%	2142	42.3	221
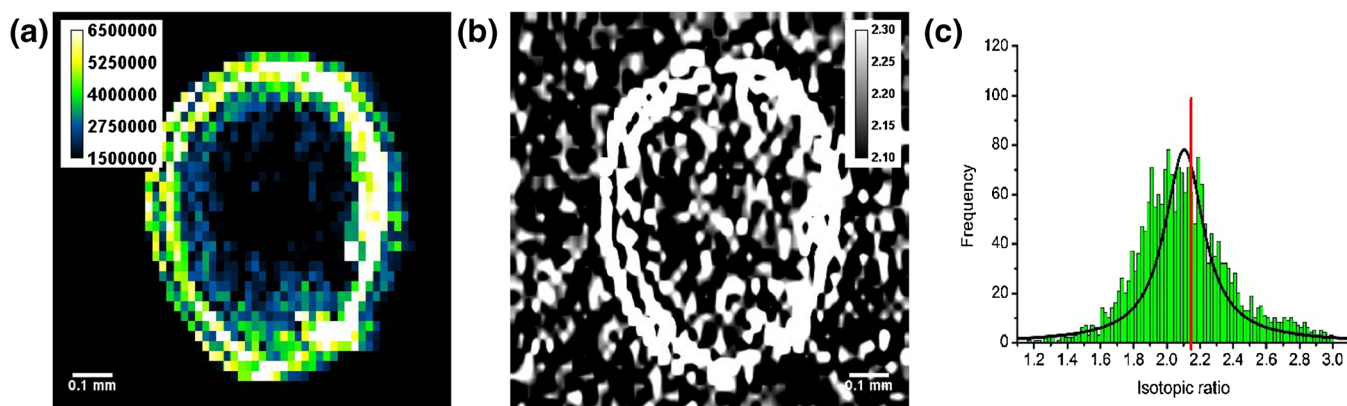
Figure 4. Results of the ablation of a dried human whole blood droplet in 56 line scans spiked with 10 mg/L lead: qualitative data for m/z 205.5–206.5 **(a)**, isotopic ratio map of $^{208}Pb/^{206}Pb$ **(b)**, and histogram of the isotopic ratio distribution (green bars, 100 center aligned bins, each 0.02), Lorentz fitting (black line) with expected natural abundance (red line) **(c)**

used for data evaluation. The duty cycle for this experiment was calculated to be 71.4% attributable to the smaller investigated mass region and the smaller spacing between the 198 recorded mass channels (about 14,256 data points per line). As before, a VBA software macro was utilized to extract the m/z traces of interest from the raw data and to add up all mass channels for one isotope. In addition, the macro is able to display the recorded isotopic pattern and to divide the results in order to generate isotopic ratio maps as in Figure3b. This can be found in the Supplementary Information.

It can be seen that not only the acquisition of an isotopic mass can be used to investigate the concentration depending distribution of trace elements but, furthermore, the isotopic pattern helps to gain more evidence about the identity of the analyte by comparing the found isotopic abundance pattern to the expected one.

However, inorganic fast survey scan acquisition imaging is also able to use the interferents as internal standards. It is even possible to do a mathematical interference correction for each pixel (i.e., to subtract the interferent signal from the analyte signal). The isotopic ratios for the dried blood sample found were plotted as a histogram with 100 bins, each with a width of 0.02. It shows how often an isotopic ratio was found for the complete image. The bars were subsequently fitted with a Lorentz curve and the maximum was compared with the natural abundance. As can be seen in Figure3c, the found ratio was in good agreement with the expected value. The width of the graph is comparably narrow and provides accurate results.

Applicability to Thin Tissue Sections

To investigate more challenging samples and to prove the capability of the fast scanning imaging approach, thin tissue slides were analyzed. Figure5 shows the isotopic pattern, which was achieved after cumulating all intensities of a single line scan over a mouse kidney after Cisplatin treatment (Figure5a). The very good agreement between the measured and the calculated isotopic pattern is obvious (Figure5b). The scan range was 190.1–200.0 u with a spacing of 0.05 u and a dwell time of

0.005s. Even the minor isotope ^{192}Pt, which has a natural abundance of 0.79%, can be detected. In addition, a meaningful Pt distribution map was obtained using the fast survey scan acquisition with a laser spot diameter of 50µm, a scan speed of 50µm/s, a repetition rate of 20Hz, and a laser energy of 1.95mJ/ shot. In the generated image for ^{195}Pt (m/z 194.5–195.5 u, sum
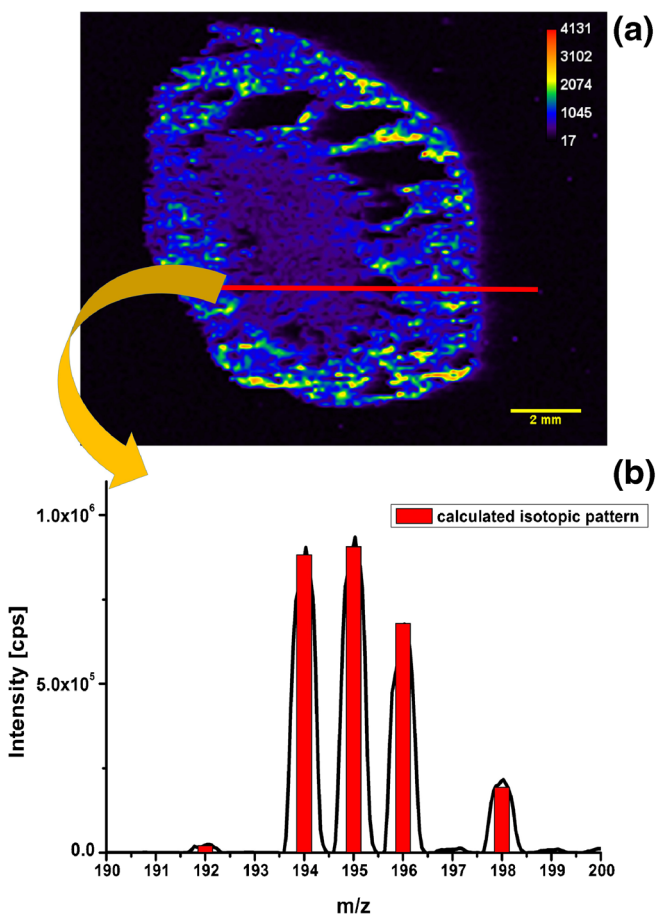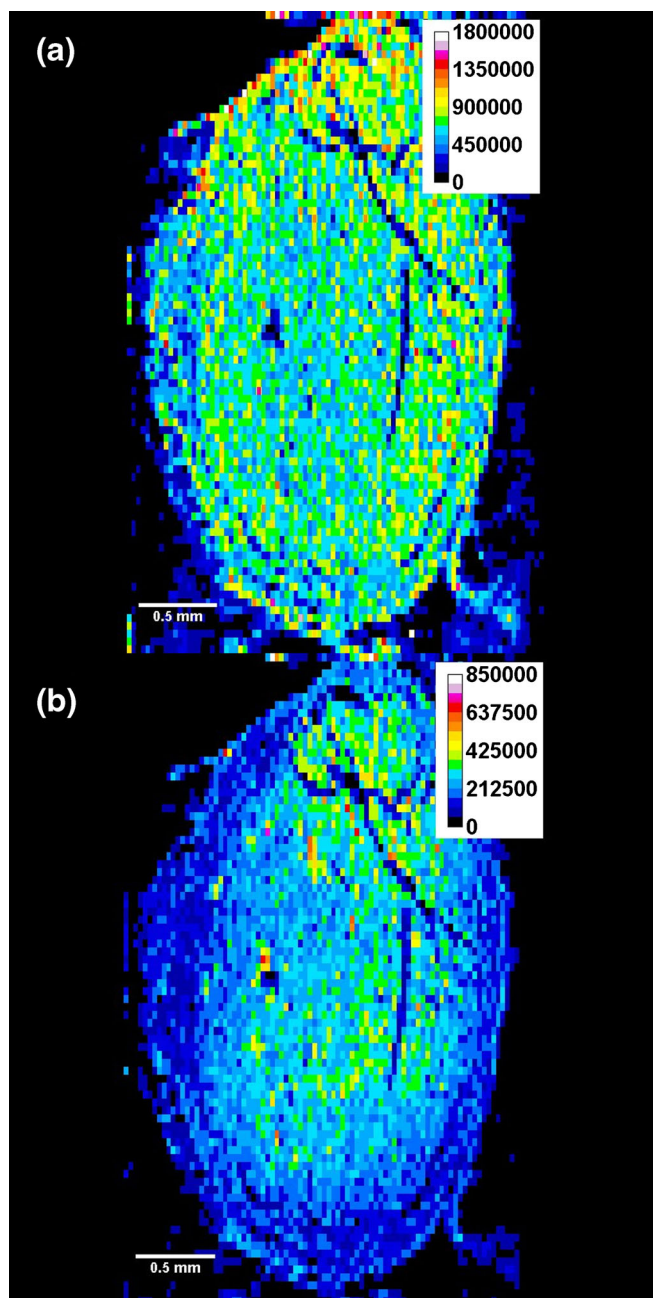

Figure 5. Ion image for ^{195}Pt of mouse kidney after Cisplatin treatment **(a)** and cumulated isotopic pattern (black line) with simulated natural abundance (red bars) for a single line scan **(b)**

of 19 mass channels) of the 3μm thick kidney section, Pt is distributed heterogeneously in the medulla inner part of the kidney, whereas an accumulation can be seen in the cortex. This result is in excellent agreement to literature, as the cortex contains the proximal tubules. They are specifically damaged after a CDDP treatment [32, 36, 37]. Additionally, an eosin Y (disodium tetrabromofluorescein) stained human lymph node was analyzed using the same instrumental conditions. This staining is commonly applied in histology to improve visualization of the thin tissue slices for microscopy. It dyes

cytoplasmic material in red color [38]. Moreover, it has been recently of interest in elemental bioimaging as a reference marker for structural information [8, 33, 39].

In Figure 6, the extracted isotopic images for ^{65}Cu (m/z 64.5-65.5) and $^{79,81}Br$ (m/z 78.5–79.5+80.5–81.5, respectively) for a human lymph node sample sectioned at 8μm are shown. The sample was ablated using a spot size of 50μm, a laser scan speed of 50μm/s, a shot repetition rate of 20Hz, and a laser energy of 2.1mJ/shot. In this case, the mass region from 43.0 to 92.0 u was investigated with a spacing of 0.1 u and a dwell time for each of 490 channels of 0.002ms. The duty cycle equaled 59.1%. The image for Cu (Figure 6a) and Br (Figure 6b) represent the sample structure well.

Conclusion

Fast survey scan acquisition was shown to be a valuable addition to the toolbox of elemental bioimaging. Advantages, including the possibility to obtain more information per image, the option to sum up mass channels, the reduction of the amount of spikes, and the increase of the sensitivity by a factor of five or even more are presented. In addition, the capability of this method to generate spatially resolved isotopic abundance maps and isotopic patterns for certain regions of the investigated samples are shown for murine kidney and human lymph node samples.

Acknowledgments

Figure 6. Images of a human lymph node sample sectioned at 8 μm and ablated with a laser spot diameter of 50 μm , showing the distribution of ^{65}Cu (m/z 64.5–65.5) and $^{79,81}Br$ (m/z 78.5–79.5, 80.5–81.5, respectively)

References

1. Wang, S., Brown, R., Gray, D.J.: Application of laser ablation-ICPMS to the spatially resolved micro-analysis of biological tissue. Appl. Spectrosc. **48**, 1321–1325 (1994)

2. Hare, D.J., Lee, J.K., Beavis, A.D., van Gramberg, A., George, J., Adlard, P.A., Finkelstein, D.I., Doble, P.A.: Three-dimensional atlas of iron, copper, and zinc in the mouse cerebrum and brainstem. Anal. Chem. **84**, 3990–3997 (2012)

3. Becker, J.S., Becker, J.S.: Mass spectrometry imaging (MSI) of metals by laser ablation ICP-MS and metallomics of biomedical samples. Biomed. Spectros. Imaging **1**, 187–204 (2012)

4. Sussulini, A., Matusch, A., Klietz, M., Bauer, A., Depboylu, C., Becker, J.S.: Quantitative imaging of Cu, Fe, Mn, and Zn in the L-DOPA-treated unilateral 6-hydroxydopamine Parkinson's disease mouse model by LA-ICP-MS. Biomed. Spectrosc. Imaging **1**, 125–136 (2012)

5. Jackson, B., Harper, S., Smith, L., Flinn, J.: Elemental mapping and quantitative analysis Cu, Zn, and Fe in rat brain sections by laser ablation ICP-MS. Anal. Bioanal. Chem. **384**, 951–957 (2006)

6. Wang, H.A.O., Grolimund, D., Giesen, C., Borca, C.N., Shaw-Stewart, J.R.H., Bodenmiller, B., Günther, D.: Fast chemical imaging at high spatial resolution by laser ablation inductively coupled plasma mass spectrometry. Anal. Chem. **85**, 10107–10116 (2013)

7. Drescher, D., Giesen, C., Traub, H., Panne, U., Kneipp, J., Jakubowski, N.: Quantitative imaging of gold and silver nanoparticles in single eukaryotic cells by laser ablation ICP-MS. Anal. Chem. **84**, 9684–9688 (2012)

8. Reifschneider, O., Wehe, C.A., Diebold, K., Becker, C., Sperling, M., Karst, U.: Elemental bioimaging of hematoxylin and eosin-stained tissues by laser ablation ICP-MS. J. Anal. At. Spectrom. **28**, 989–993 (2013)

9. Donati, G.L., Amais, R.S., Nóbrega, J.A.: Interference standard: a new approach to minimizing spectral interferences in inductively coupled plasma mass spectrometry. J. Anal. At. Spectrom. **26**, 1827–1832 (2011)

10. Longerich, H.P., Jackson, S.E., Günther, D.: Inter-laboratory note. Laser ablation inductively coupled plasma mass spectrometric transient signal data acquisition and analyte concentration calculation. J. Anal. At. Spectrom. **11**, 899–904 (1996)

11. Hieftje, G.M., Barnes, J.H., Gron, O.A., Leach, A.M., McClenathan, D.M., Ray, S.J., Solyom, D.A., Wetzel, W.C., Denton, M.B., Koppensaal, D.W.: Evolution and revolution in instrumentation for plasma-source mass spectrometry. Pure Appl. Chem. **73**, 1579–1588 (2001)

12. Römpp, A., Spengler, B.: Mass spectrometry imaging with high resolution in mass and space. Histochem. Cell Biol. **139**, 759–783 (2013)

13. Seeley, E.H., Schwamborn, K., Caprioli, R.M.: Imaging of intact tissue sections: moving beyond the microscope. J. Biol. Chem. **286**, 25459–25466 (2011)

14. Tanner, M., Günther, D.: Signal acquisition in μs time resolution for intorch LA-ICP-MS. J. Anal. At. Spectrom. **22**, 1189–1192 (2007)

15. Laborda, F., Medrano, J., Castillo, J.R.: Estimation of the quantification uncertainty from flow injection and liquid chromatography transient signals in inductively coupled plasma mass spectrometry. Spectrochim. Acta Part B **59**, 857–870 (2004)

16. Venable, J.D., Langer, D., Holcombe, J.A.: Optimizing the multi-element analysis capabilities of an ICP quadrupole mass spectrometer using electrothermal vaporization sample introduction. Anal. Chem. **74**, 3744–3753 (2002)

17. Schilling, G.D., Andrade, F.J., Barnes IV, J.H., Sperline, R.P., Denton, M.B., Barinaga, C.J., Koppenaal, D.W., Hieftje, G.M.: Continuous simultaneous detection in mass spectrometry. Anal. Chem. **79**, 7662–7668 (2007)

18. Vanhaecke, F., Moens, L., Dams, R.: Precise measurement of isotope ratios with a double-focusing magnetic sector ICP mass spectrometer. Anal. Chem. **68**, 567–569 (1996)

19. Urgast, D.S., Feldmann, J.: Isotope ratio measurements in biological tissues using LA-ICP-MS–possibilities, limitations, and perspectives. J. Anal. At. Spectrom. **28**, 1367–1371 (2013)

20. Urgast, D.S., Ou, O., Gordon, M.-J., Raab, A., Nixon, G.F., Kwun, I.-S., Beattie, J., Feldmann, J.: Microanalytical isotope ratio measurements and elemental mapping using laser ablation ICP-MS for tissue thin sections: zinc tracer studies in rats. Anal. Bioanal. Chem. **402**, 287–297 (2012)

21. Flórez, M.R., Aramendía, M., Resano, M., Lapeña, A.C., Balcaen, L., Vanhaecke, F.: Isotope ratio mapping by means of laser ablation-single collector-ICP-mass spectrometry: Zn tracer studies in thin sections of *Daphnia magna*. J. Anal. At. Spectrom. **28**, 1005–1015 (2013)

22. Mahoney, P.P., Li, G.Q., Hieftje, G.M.: Laser ablation-inductively coupled plasma mass spectrometry with a time-of-flight mass analyzer. J. Anal. At. Spectrom. **11**, 401–405 (1996)

23. Borovinskaya, O., Hattendorf, B., Tanner, M., Gschwind, S., Günther, D.: A prototype of a new inductively coupled plasma time-of-flight mass spectrometer providing temporally resolved, multi-element detection of short signals generated by single particles and droplets. J. Anal. At. Spectrom. **28**, 226–233 (2013)

24. Bandura, D.R., Baranov, V.I., Ornatsky, O.I., Antonov, A., Kinach, R., Lou, X., Pavlov, S., Vorobiev, S., Dick, J.E., Tanner, S.D.: Mass cytometry: technique for real time single cell multitarget immunoassay based on inductively coupled plasma time-of-flight mass spectrometry. Anal. Chem. **81**, 6813–6822 (2009)

25. Olesik, J.W., Gray, P.J.: Considerations for measurement of individual nanoparticles or microparticles by ICP-MS: determination of the number of particles and the analyte mass in each particle. J. Anal. At. Spetrom. **27**, 1143–1155 (2012)

26. Shigeta, K., Traub, H., Panne, U., Okino, A., Rottmann, L., Jakubowski, N.: Application of a micro-droplet generator for an ICP-sector field mass spectrometer —optimization and analytical characterization. J. Anal. At. Spetrom. **28**, 646–656 (2013)

27. Gschwind, S., Flamigni, L., Koch, J., Borovinskaya, O., Groh, S., Niemax, K., Günther, D.: Capabilities of inductively coupled plasma mass spectrometry for the detection of nanoparticles carried by monodisperse microdroplets. J. Anal. At. Spetrom. **26**, 1166–1174 (2011)

28. Leach, A.M., Hieftje, G.M.: Factors affecting the production of fast transient signals in single shot laser ablation inductively coupled plasma mass spectrometry. Appl. Spectrosc. **56**, 62–69 (2002)

29. Grimm, C.C., Clawson, R., Short, R.T.: Use of region II of the a/q stability diagram for fast scanning of a linear quadrupole mass spectrometer. J. Am. Soc. Mass Spectrom. **8**, 539–544 (1997)

30. Tanner, M., Günther, D.: Short transient signals, a challenge for inductively coupled plasma mass spectrometry, a review. Anal. Chim. Acta **633**, 19–28 (2009)

31. Pettke, T., Heinrich, C.A., Ciocan, A.C., Günther, D.: Quadrupole mass spectrometry and optical emission spectroscopy: detection capabilities and representative sampling of short transient signals from laser-ablation. J. Anal. At. Spetrom. **15**, 1149–1155 (2000)

32. Furuta, N.: Optimization of the mass scanning rate for the determination of lead isotope ratios using an inductively coupled plasma mass spectrometer. J. Anal. At. Spectrom. **6**, 199–203 (1991)

33. Herdering, C., Wehe, C.A., Reifschneider, O., Raj, I., Ciarimboli, G., Diebold, K., Becker, C., Sperling, M., Karst, U.: Laser ablation based bioimaging with simultaneous elemental and molecular mass spectrometry: towards spatially resolved speciation analysis. Rapid Commun. Mass Spetrom. **27**, 2588–2594 (2013)

34. Lear, J., Hare, D., Adlard, P., Finkelstein, D., Doble, P.: Improving acquisition times of elemental bio-imaging for quadrupole-based LA-ICP-MS. J. Anal. At. Spetrom. **27**, 159–164 (2012)

35. Tanner, M.: Shorter signals for improved signal to noise ratio, the influence of Poisson distribution. J. Anal. At. Spectrom. **25**, 405–407 (2010)

36. Townsend, D.M., Deng, M., Zhang, L., Lapus, M.G., Hanigan, M.H.: Metabolism of Cisplatin to a nephrotoxin in proximal tubule cells. J. Am. Soc. Nephrol. **14**, 1–10 (2003)

37. Moreno-Gordaliza, E., Giesen, C., Lazaro, A., Esteban-Fernandez, D., Humanes, B., Canas, B., Panne, U., Tejedor, A., Jakubowski, N., Gomez-Gomez, M.M.: Elemental bioimaging in kidney by LA-ICP-MS as a tool to study nephrotoxicity and renal protective strategies in Cisplatin therapies. Anal. Chem. **83**, 7933–7940 (2011)

38. Horobin, R.W., Kiernan, J.A. Conn's biological stains: A handbook of dyes, stains, and fluorochromes for use in biology and medicine. BIOS Scientific Publishing, Oxford (2002)

39. Herdering, C., Reifschneider, O., Wehe, C.A., Sperling, M., Karst, U.: Ambient molecular imaging by laser ablation atmospheric pressure chemical ionization mass spectrometry. Rapid Commun. Mass Spectrom. **27**, 2595–2600 (2013)